

MANOEVRE-LOADS COMPUTATIONS USING CFD-BASED STATIC AEROELASTIC SIMULATIONS FOR MULTIPLE STORE CONFIGURATIONS

B.B. Prananta, R.P.G. Veul and O.J. Boelens
National Aerospace Laboratory NLR

Keywords: manoeuvre loads, aeroelastic simulation, computational fluid dynamics

Abstract

The paper presents a modular manoeuvre-loads computation method based on a static aeroelastic simulation applicable for multiple store configurations. The aerodynamic loads are computed using a structured multi-block CFD method, taking into account structural deformation. Practical limitation of structured multi-block CFD methods, namely the unacceptably long grid generation for complex configuration, is overcome by using modular approach per store station. A non-matching boundary method is used between store stations. A trimmed condition, achieved by deflecting the control surfaces, is sought during the analysis to obtain balance loads. Significant gain in turn around time with adequate accuracy is obtained.

1 Introduction

Knowledge of the actual manoeuvre loads is of paramount important to support effective operations of military aircraft. This is especially true for a multi-role combat aircraft which can be deployed for various types of mission with loads-spectrum differs significantly from the assumed spectrum during the design stage. A large part of this unprecedented loads spectrum is related to new type of stores or new store configurations. The knowledge of actual loads can be used for designing fit-for-the usage maintenance of an aircraft and improving fleet deployment.

Loads data are usually obtained through a combination of post-flight (health monitoring) [2] and pre-flight (analytical prediction)

methods [3]. The proposed paper focuses on an accurate and efficient loads prediction method using a computational fluid dynamic (CFD) based static aeroelastic simulation suitable for multiple store configurations.

An overview of the NLR loads prediction method has been presented in detail in Ref. [4]. The method is built around a multi-parameter loads database with carefully defined support points called the point-in-the-sky (PITS). Data in a PITS represent realistic loads for a predefined flight condition and aircraft configuration. The following characteristics are therefore inherent in the PITS data: balance between the aerodynamic and the inertia loads, trimmed condition satisfying the flight control system law, correct fuel distribution for a certain fuel level and correct mass distribution of stores. The loads data for a PITS is obtained using a static aeroelastic simulation employing a carefully selected combination of high fidelity and low fidelity computational models. For flight conditions at a transonic Mach number and/or a high normal load factor, an advanced aerodynamic model based on CFD is applied. The in-house developed CFD method of NLR, the ENFLOW system, is employed for this purpose.

The underlying numerical method of the ENFLOW system is based on structured multiblock grid approach. It consists of ENSOLV flow solver, ENDOMO domain modeller and ENGRID grid generator, see e.g. Ref. [10].

Efficient use of a CFD method based on structured multiblock grids for computation of manoeuvre loads is hampered by the complexity of grid generation around stores. In the past

years National Aerospace Laboratory NLR has developed an efficient structured multi-block grid generation method based on a novel Cartesian block decomposition technique [1]. Turn around time of generating grid around a complex military aircraft with complex store configuration has been reduced substantially. However, when considering a military aircraft with very large possibilities of store configurations, grid generation will still be a bottleneck.

The objective of the present study is therefore to devise a static aeroelastic simulation method capable of handling multiple store configurations with ease. As the bottleneck of the current method has been identified, the work focuses on the grid strategy.

In the present study, a new approach is introduced using a modular technique. Grid generation for each store station is carried out independently from each other for a predefined rectangular domain. The topology at the domain boundary does not need to be properly connected. This implies that one-to-one grid connection at the domain boundary is not required, improving the modularity of the approach significantly. A non-matching block coupling method is developed in ENSOLV to couple these domains. In the present study, a non-matching block boundary approach with a predefined interface is preferred above a more commonly used overlapping grid method due to its simplicity and its relatively limited modification to current method. Having a predefined interface, instead of on-the-fly-computed interface like in the case of overlapping grid method, has not been found as a limiting factor.

A non-matching block boundary approach has been applied mostly for simulations of a multistage turbo machine, counter rotating rotors and helicopter blade-fuselage interaction. Application of such a method for aeroelastic simulation has never been reported since it requires careful grid deformation management. As in the case of Chimera method, strict conservation of the method is not maintained between the domains. However, based on preliminary results, adequate accuracy is obtained.

In this paper the method will be elaborated further, verification test cases with LANN wing will be presented and finally a realistic test case of static aeroelastic simulations of a fighter aircraft with stores will be shown. Since the present static aeroelastic simulation method has been presented elsewhere, e.g. Ref. [3][4], only modifications related to the present modular approach will be discussed.

2 Modular grid generation

It is generally known that generating a structured multiblock grid around a relatively complex configuration is extremely labour intensive. Moreover, it requires a high level of experience leaving such activity only suitable for dedicated persons. Fig. 1 shows an example of block arrangement of an Euler grid around a fighter aircraft with stores, generated about two decades ago almost completely manually using the domain modeller ENDOMO.

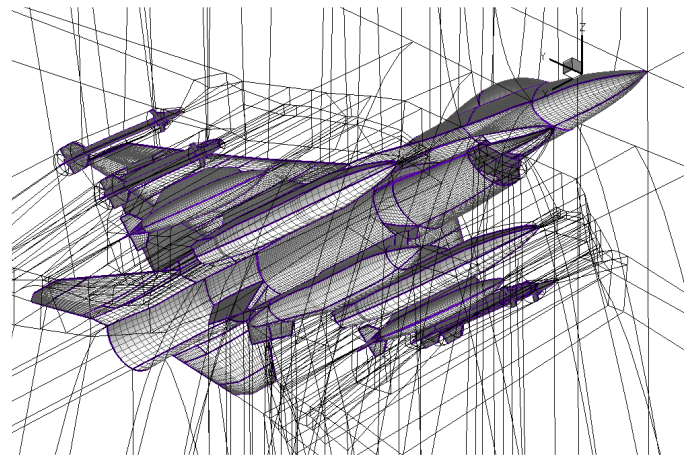


Fig. 1 Example of block arrangement around a fighter aircraft with various stores for flow simulation employing Euler modelling

It took about two months to generate this grid with 450 blocks. Significant geometry simplifications were carried out and many undesirable singularities had to be introduced in the topology to keep the work tractable. At the time the grid was generated, RANS grid was considered too complex for this configuration.

Since then, NLR has made significant progress in structured multiblock grid generation with the development of a novel semi-automatic block decomposition method

called the Cartesian block mapping method, see e.g. Refs. [1][8]. Fig. 2 shows an example of the block arrangement of a RANS grid around an F-16 XL model generated using this approach.

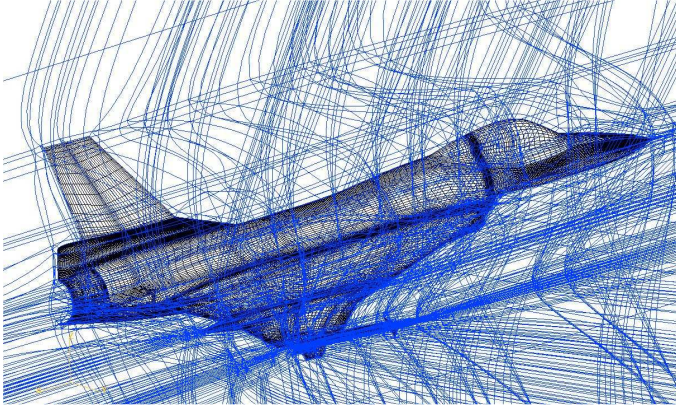


Fig. 2 Example of a complex block-arrangement around an F-16 XL aircraft model with a high geometric detail, from Ref.[1]

This grid has about 2000 blocks representing half configuration of the F-16 XL and was generated in less than two weeks. Almost all geometrical details are taken into account, i.e. the split between the inlet and the fuselage, the inlet duct up to the engine fan, the air dam, the actuator pod, the missile and the fins of the missiles. The large number of blocks are necessary to have a good control on the generated grids and can be merged afterwards to gain a better computing performance on a vector computer. The grid was used in the successful CAWAPI project, Ref. [1][9].

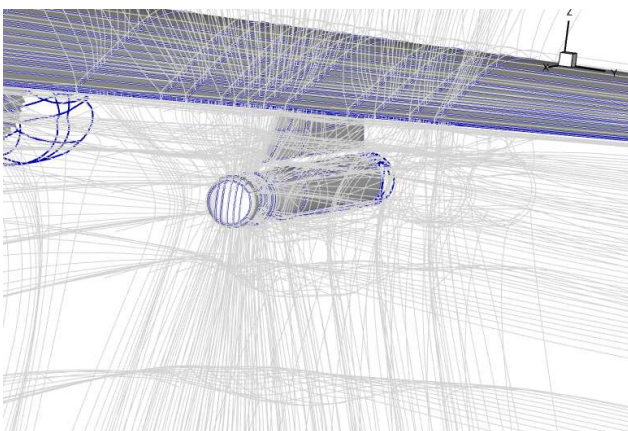


Fig. 3 Part of the block arrangement about a military transport aircraft with stores, from Ref. [8]

Despite this significant development, generating grid for a configuration with many types of store is still considered time consuming. An example is the grid about a military transport aircraft used in Ref. [8] which includes an engine pylon, a nacelle, a propeller disk, a torpedo at the inner wing station and a depth charge at the outer wing station. Part of the block arrangement is shown in Fig. 3. Inherent to the concept of structured multiblock grid method, the topology of a store must have a proper connection with the other parts of the geometry. This increases the already-strong dependency of one part to the other parts of the grid to a level that can easily become unmanageable.

A modular approach is therefore proposed to handle the grid generation of aircraft with many combinations of stores. Basically, the approach can be summarised as:

1. simplification of block decomposition by removing the topological dependency of a complicated part to other parts of the grid,
2. reuse of a topological part for different combinations with other parts.

The first approach confines the complexity of the topology of a part inside a domain reserved for this part. The consequence of the first approach is that the interface between parts of the grid will not be topologically compatible. In turn, the grid at the interface will also be different between parts. This consequence requires the use of a non-matching block boundary approach in the flow solver. The second approach will allow quick and efficient storage and generation of a grid for a certain store configuration. The consequence, is that the interface of a part should be made as standard as possible.

To clarify this approach, the method is applied to a multi role fighter aircraft. The aircraft has nine store attachment stations, numbered as station 1 at the tip of the port-side wing, up to station 9 at the tip of the starboard wing. Fig. 4 shows the part of block arrangement for the starboard half of the aircraft. Station 5, i.e. under the fuselage, is assumed to be empty. The grid is divided into nine parts. The main part, upper figure of Fig. 4, contains the fuselage and the tails. For each

wing station a separate part is constructed holding a part of the wing and the desired store. In this example only station 6 at the inner wing has a store, i.e. a 370 lb external fuel tank. It can be seen that rectangular faces are selected for the interface boundaries of the grid parts. This represents the aforementioned standard interface for this configuration to facilitate grid part interchange for various types of store.

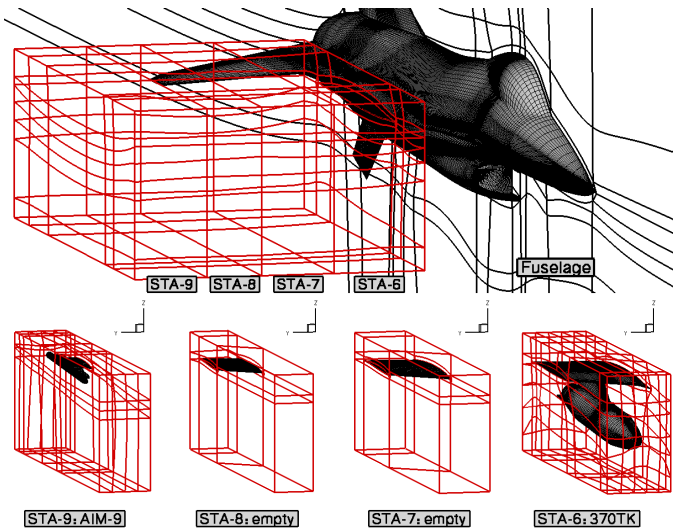


Fig. 4 Overview of the modular aerodynamic store modelling. In the main part of the aircraft model, i.e. upper figure, four holes are reserved in its domain to be filled in with domains containing the desired stores at various stations, shown in the lower part of the figure.

For each station, grids for several types of store can be generated independently. Fig. 5 shows the surface grid and interface boundary for two types of store at station 7, i.e. an AMRAAM missile (left figure) and a 1000 lb class bomb Mark 84 (right figure).

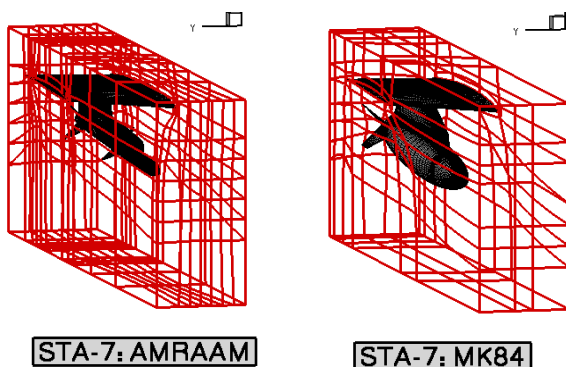


Fig. 5 Example of other possible stores for station 7, i.e. AMRAAM missile (left) and Mark 84 bomb

The fact that the topology for these parts of the grid does not have to match with other parts, gives freedom in deciding on the level of complexity of this part. In this case, it is opted for a moderate degree of detail. Fig. 6 shows a more detailed view of the block arrangement around an AMRAAM missile attached at station 7.

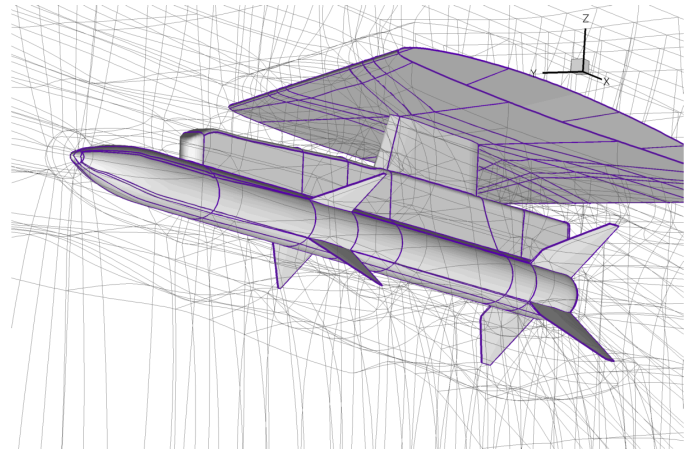


Fig. 6 Overview of block arrangement in station 7 domain around an AMRAAM missile, the modular approach allows more details to be included with ease

3 Non-matching block coupling method

To facilitate the modular grid generation, a non-matching block coupling has to be developed for the ENFLOW system. The flow solver of the ENFLOW system, ENSOLV, applies a cell-centred finite volume method. The set of conservative variables, assuming a $k-\omega$ type turbulence model is used, $Q = [\rho, \rho u, \rho v, \rho w, \rho E, \rho k, \rho \omega]$ is therefore stored in the centre of the computation cells.

The communication between two adjacent blocks having perfectly matched block faces is carried out using two layers of ghost cells. The value of the flow variables in the ghost cells of the present block is simply copied from the flow variables of the neighbouring blocks, i.e.

$$Q^G = Q^N, \quad (1)$$

where Q^G is the flow variables at the ghost cells of the present block and Q^N is the flow variables of the neighbouring block at locations which are compatible with the ghost cells of the present

block. When the block faces are not matched, prior to copying the flow variables, an interpolation process has to be carried out in the neighbouring blocks to obtain the value of the flow variables at locations compatible with the ghost cells of the present block.

Various interpolation procedures can be applied at the boundary. The choice is down to whether the structure of the data will be used. Since it is desired that a group of block faces will be interpolated at once, if the structure of the data is kept, a book keeping procedure has to be introduced. Here, a method with the simplest book keeping is preferred. An interpolation method belongs to the class of scattered data interpolation methods is therefore used, see e.g. Ref.[6]. A scattered data interpolation method using radial basis functions is applied as,

$$Q^N(\bar{x}) \approx \bar{Q}(\bar{x}) = P(\bar{x}) + \sum a_i \phi_i(|\bar{x} - \bar{x}_i|), \quad (2)$$

where the over-bar indicates an approximation, $P(\bar{x})$ is a low order polynomial, ϕ_i is the i -th radial basis function and x_i is the location of the i -th support point of the approximation. Regarding the selection of $P(\bar{x})$ and ϕ , the first option is to employ the volume spline of Ref. [5] which uses a zeroth order polynomial and a biharmonic type radial basis function. The approximation function becomes

$$\bar{Q}(\bar{x}) = p_0 + \sum a_i |\bar{x} - \bar{x}_i|, \quad (3)$$

where the summation runs on all support points. For the present application, the approximation coefficients, p_0 and a_i , can be computed by evaluating Eq. (3) at $j=1..n^N$ cell-centres of the neighbouring block to arrive to,

$$p_0 + \sum a_i |\bar{x}_j - \bar{x}_i| = Q_j, \quad (4)$$

completed with an equilibrium condition,

$$\sum a_i = 0. \quad (5)$$

The summation in Eq. (4) and Eq. (5) runs on all cell centres of the neighbouring block, i.e. $i=1..n^N$. The set of (n^N+1) linear equations, Eq. (4) and Eq. (5), can be solved for each member of the flow variables to obtain the approximation coefficients, p_0 and a_i . With these coefficients, the flow variables at the ghost cells of the present block can be computed using Eq. (3).

The aforementioned steps can be re-arranged to have a direct relation between the flow variables at the ghost cells and the flow variables at the neighbouring block as,

$$Q^G = [G_{GN}] Q^N. \quad (6)$$

The subscript GN indicates that the interpolation matrix $[G_{GN}]$ is obtained by evaluating Eq. (3) for the N -set support point at the neighbouring block and is used to compute the G -set values at the ghost cells of the present block. A detailed description on how to compute the interpolation matrix $[G_{GN}]$ is presented in Ref. [5]. Note that the interpolation matrix $[G_{GN}]$ depends only on the coordinates of the ghost cells of the present block and the coordinates of the cell-centres of the neighbouring block. Thus it needs to be computed only once and can be used for each member of the flow variables. The interpolation matrix has to be updated only when the grid deforms, e.g. during an aeroelastic simulation.

In a fluid structure interaction procedure, the interpolation method with radial basis functions is used to transfer the deformation from the structural model to the aerodynamic model as, Ref.[5][11]

$$d\bar{x}^A = [G_{AS}] d\bar{x}^S. \quad (7)$$

To ensure the conservation of virtual energy, the transfer of the aerodynamic forces to the structural model uses the transpose of the interpolation matrix as

$$\vec{F}^S = [G_{AS}]^T \vec{F}^A. \quad (8)$$

In fact using Eq. (8) to transfer the aerodynamic forces also ensures that the total force is exactly preserved between the aerodynamic and the structural models because the interpolation method satisfies the equilibrium condition, i.e. Eq. (5). If, instead of a zeroth order, a first order polynomial is used for the interpolation approximation in Eq.(2), i.e.

$$P(\bar{x}) = p_0 + p_1x + p_2y + p_3z, \quad (9)$$

the preservation of the total moment between the structural and the aerodynamic models is also ensured. In this case, in addition to Eq. (5) the following equilibrium conditions have to be satisfied:

$$\begin{aligned}\Sigma a_i x &= 0, \\ \Sigma a_i y &= 0, \\ \Sigma a_i z &= 0.\end{aligned}\quad (10)$$

Note that the fundamental property of interpolation methods using radial basis functions, Eq. (2), is that it provides a continuous and sufficiently smooth representation of irregularly positioned data. It means that the data to be interpolated should have a sufficient smoothness, see e.g. Ref. [6]. The method is therefore applicable for data such as: a deformation field, a pressure distribution or, in the case of the present block coupling, flow variables. Eq. (8), on the other hand, is applicable for integrated/discrete quantities, for examples forces, integrated about a certain area, or mass, integrated about a certain volume. Method based on Eq. (8) has been successfully applied in Ref. [7] to map concentrated mass data between two finite element models while preserving the total mass.

Borrowing the idea from transferring the forces in a fluid structure interaction procedure, a conservative transfer of flow variables across non-matching block boundaries can be devised. Eq. (8) is applied to transfer the flow variables weighted with the cell area as,

$$Q^G = [h^G]^{-1} [G_{NG}]^T [h^N] Q^N, \quad (11)$$

where $[h]$ is a diagonal matrix with the area of the cells at the block face in its diagonal. Note that the interpolation matrix $[G_{NG}]$ is now evaluated at the ghost cells of the present block.

Both types of interpolation, i.e. Eq. (6) and Eq. (11), have been implemented in ENSOLV. Based on preliminary results, however, it is found that the conservative interpolation Eq. (11) is much less robust than Eq.(6), especially when the area distributions are significantly different between the non-matching block boundaries. Further research is therefore still required, especially in selecting the proper radial basis function ϕ for the conservative interpolation method. All results presented in this paper are obtained using an interpolation method based on Eq.(6).

To obtain the interpolation matrix, an inversion of a full-matrix is required. The size of the matrix depends on the number of cells at

the block boundaries which can be relatively large. This can potentially be a limitation in terms of computing time. Therefore, an option to use only a limited number of support points in the nearest neighbourhood of a ghost cell is also implemented.

4 Fluid structure interaction and grid deformation method

To maximise the modularity of the proposed approach, during a static aeroelastic simulation involving a computational grid with many parts, each part is treated independently. A method to synchronise these parts during the simulation is therefore needed, especially regarding the surface and volume grid deformation.

The basic principle of the method is that the deformation is treated hierarchically. The prime source of the deformation is the structural model. The deformation of the structural model is mapped to the aerodynamic surface through a fluid structure interaction procedure. Subsequently, the deformation of the aerodynamic surface grid defines the deformation of the block boundaries through a block boundary deformation procedure. Note that a block boundary consists of six block faces surrounded by 12 edges. The deformation of a block boundary can also be treated hierarchically, i.e. the deformation of the edge defines the deformation of the face. Finally, the deformation of the block boundary defines the deformation of volume grid inside the block.

For each level in the hierarchy any deformation method can be selected independently. With regard to the present modular approach the following requirements have to be satisfied:

1. the surface deformation at the boundary of the connecting parts has to be the same,
2. the deformation of the block boundaries participating in a non-matching block coupling has to be the same.

Satisfaction of these requirements is explained below.

The fluid structure interpolation applied in the ENFLOW system uses a volume spline method, i.e. Eq. (2). To satisfy the first

requirement all points in the structural model have to be used for all aerodynamic surface grid, even for the store parts.

The default block boundary deformation method uses a volume spline to deform the edges of the block boundary and a transfinite interpolation to deform the face of the block boundary based on the deformation of the edges, see Ref. [12]. To satisfy the second requirement, the same support points have to be used for the volume spline to deform the edges of the block boundaries. In practice a very small number of support points are enough to define the deformation of the edges. The minimum set of the support point is all aerodynamic surface points connected to the edge of the block boundary.

5 Verification case of LANN wing

To verify the present modular grid approach, the well known AGARD test case of LANN wing is used. The CT5 case involving strong shockwave boundary layer interaction is selected with a Mach number of 0.82, an angle-of-attack of 0.60 deg and a Reynolds number of 7.3 millions. First, computations are carried out on a modular grid derived from a single grid to verify that the method should revert to an exact solution when the block boundaries are perfectly matched. The accuracy of using a limited support points to reduce computing time will be investigated. Next, computations using modular grid with non-matching boundary are performed to test the performance of the method.

The grid used for the first computations is shown in Fig. 7. This grid is actually generated as a single grid but then divided into 3 parts as shown in this figure, for the purpose of verifying the proposed method. Preliminary computations using RANS and Euler flow modelling are carried out without employing the modular approach. The results are shown in Fig. 8 along with the experimental data of NLR. It can be seen that the Euler results produce shockwaves which are way too strong, suggesting that a strong shockwave-boundary layer interaction occurs during the experiment. The results with RANS flow modelling show significant

improvement. These results are used as a reference for the computations to follow.

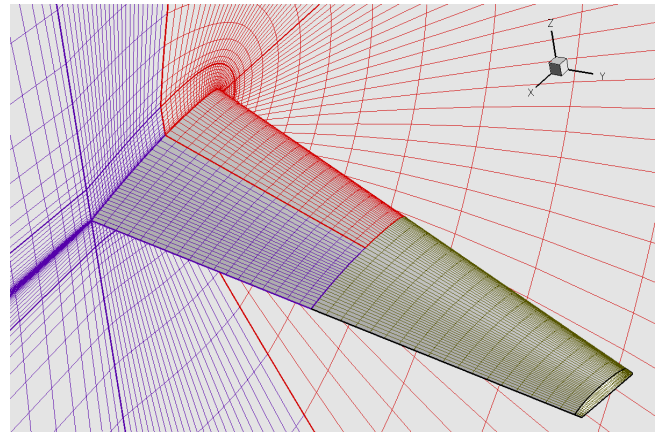


Fig. 7 Overview of the RANS grid around LANN wing with 3 domains used for verification test case

Subsequently, two computations are carried out using the proposed modular approach with the volume spline interpolation at the non-matching boundaries.

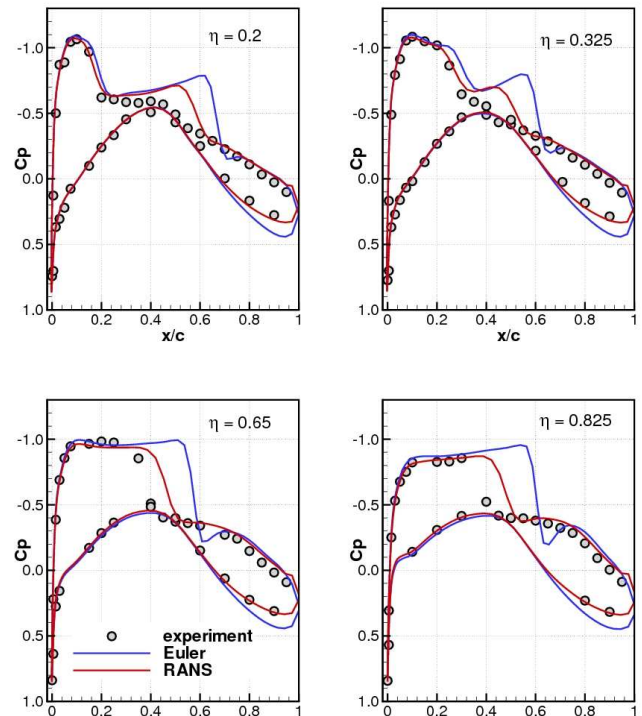


Fig. 8 Results of computation using RANS and Euler flow modelling on a single grid used as reference for a LANN wing boundary at Mach 0.82, angle-of-attack 0.60 deg and Reynolds number 7.3 millions

One computation uses all cells at the boundary as support points for the interpolation and another computation uses only 10 nearest cells

as support points for the interpolation. The use of only 10 nearest cells as support points reduces the computing time for the interpolation significantly. Comparison of the contours of surface pressure between modular and single grid approach is shown in Fig. 9. For a perfectly matched block boundary the interpolation should give exact value of the interpolated quantities. This is a property of the employed volume spline method. As can be seen in Fig. 9 the results in terms of surface pressure contours are indeed the same.

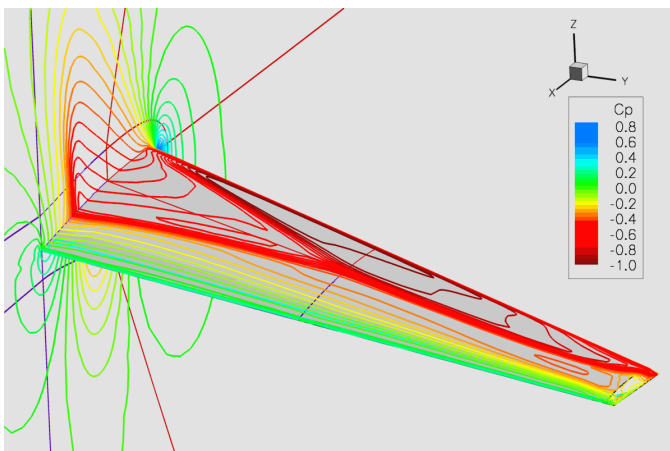


Fig. 9 Comparison of the contours of surface pressure of LANN wing between modular (dashed-line) and single grid approach (solid-line) for perfectly matched block boundary at Mach 0.82, angle-of-attack 0.60 deg and Reynolds number 7.3 millions, exactly the same results are obtained

The detailed plot of surface pressure at several sections along the span, shown in Fig. 10 gives similar conclusion.

Two computations are now carried out using a modular grid having non-matching boundary. To expose the differences better, relatively coarse grids are used in combination with computations using Euler flow modelling. First computation is performed on a grid with similar grid density at the boundary but with a different distribution. The second computation is performed on a grid with a different stretching in addition to the different density at the boundary. The overview of the latter grid is shown in Fig. 11. The results in terms pressure distribution at several sections along the span is shown in Fig. 12. Only very small differences are observed between the results.

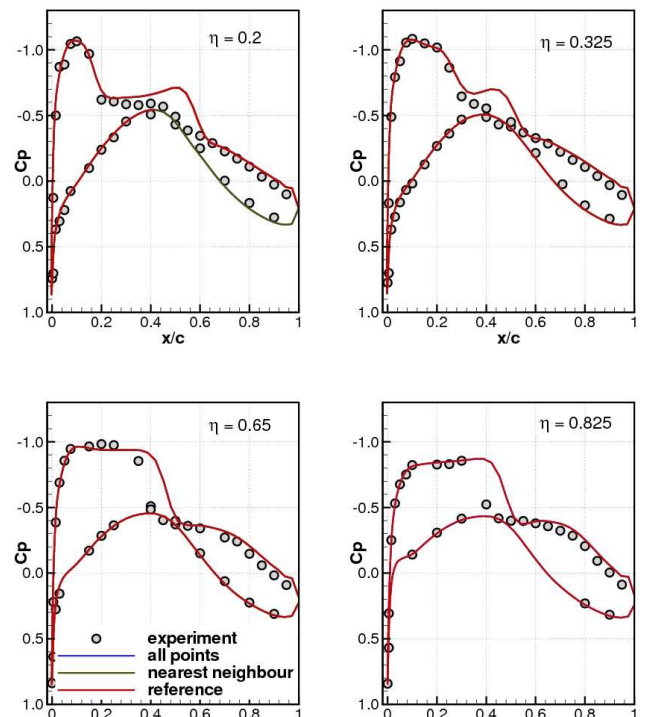


Fig. 10 Comparison of the pressure at several sections of LANN wing between modular and single grid approach) for perfectly matched block boundary at Mach 0.82, angle-of-attack 0.60 deg and Reynolds number 7.3 millions, exactly the same results are obtained

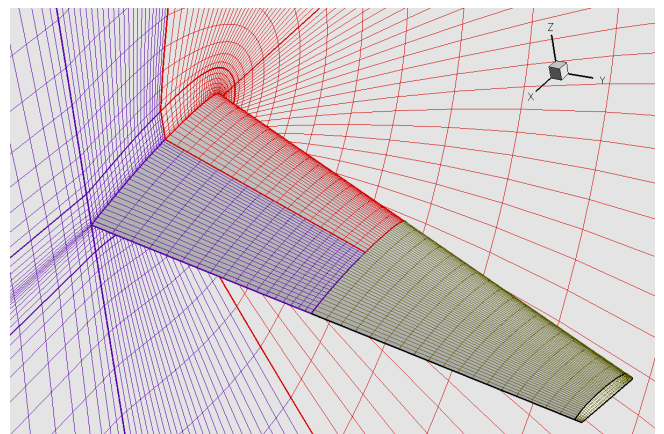


Fig. 11 Overview of the Euler grid around LANN wing with 3 domains having discontinuity at the boundary used for verification test case

The small differences are mostly found between the reference results and the results obtained using the modular grids with discontinuity, i.e. different stretching, at the boundary. Fig. 13 gives a better view on the differences by comparing the surface pressure contours. It can be mentioned, however, that the magnitude of

these differences is quite normal for computations using different single grids.

From the exercise presented in this section, it can be concluded that the present modular grid method has been verified to give adequate accuracy.

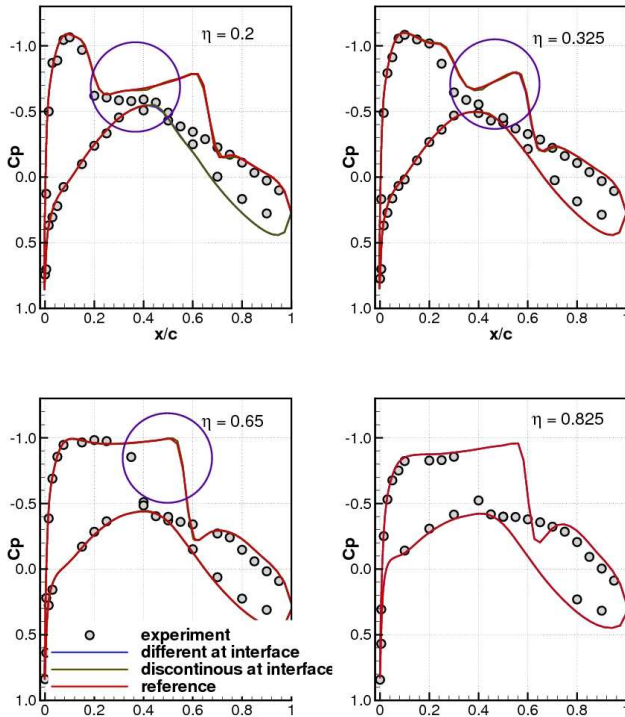


Fig. 12 Comparison of the pressure at several sections of LANN wing between modular and single grid approach) for non-matching block boundary at Mach 0.82, angle-of-attack 0.60 deg and Reynolds number 7.3 millions

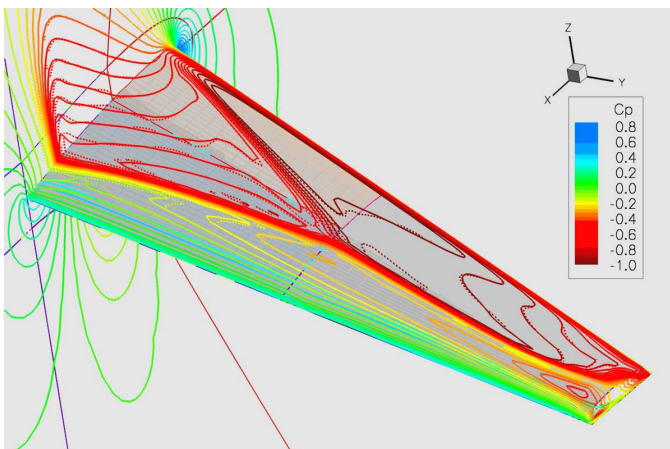


Fig. 13 Comparison of the contours of surface pressure of the LANN wing between modular (dashed-line) and single grid approach (solid-line) for discontinuous block boundary at Mach 0.82,

angle-of-attack 0.60 deg and Reynolds number 7.3 millions, only a limited differences are observed

6 Application to fighter aircraft with stores

Real life applications of a fighter aircraft in transonic flow are now presented. First the results between single grid approach and modular grid approach are compared for a store configuration consisting of external fuel tanks at station 4 and 6, empty weapon pylons at station 3 and 7, dummy missiles (also known as training missiles) at station 1 and 9 and a reconnaissance pod at station 5. The single grid for this configuration has been generated earlier in other project. For the modular grid only the grid at station 6 needs to be generated and then assembled with the main grid and grids for other stations, as already shown in Fig. 4. The time required to generate the single grid is about twice, if all components of the modular grid are taken into account, and about eight times if only the grid at station 6 needs to be generated.

The computation is performed at Mach 0.755 and angle-of-attack 3 deg. Fig. 14 shows the results in terms of surface pressure distribution, where starboard part is computed using single grid while the port-side part using present modular approach. The modular grid approach follows the division according to Fig. 4.

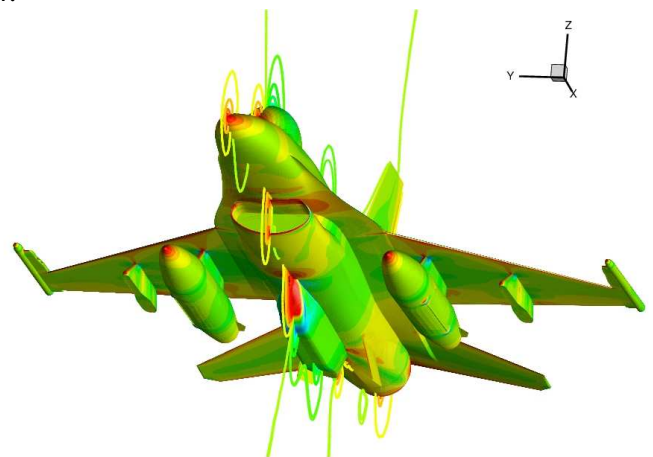


Fig. 14 Overview of pressure distribution around a fighter aircraft with external fuel tank at station 4 and 6, empty weapon pylon at station 3 and 7 and dummy missiles at station 1 and 9, at Mach 0.755 and angle-of-attack 3 deg, starboard part is computed using single grid while the port-side part using present modular approach

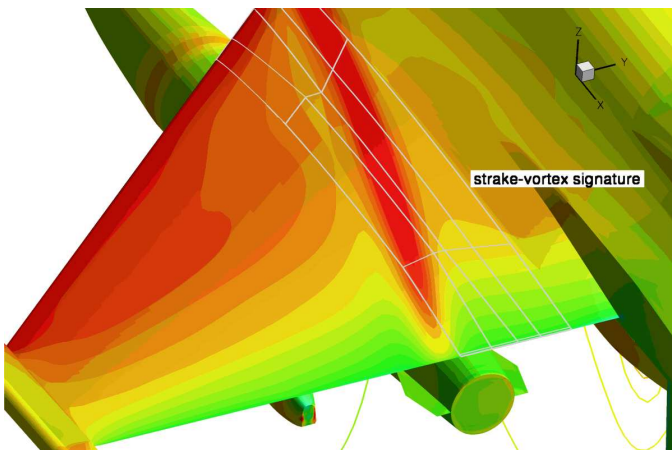


Fig. 15 Pressure distribution on the wing with a signature of the strake vortex showing the ability of the present modular approach to preserve important flow feature across non-matching boundary

Similar results are obtained between the port-side and starboard part of the aircraft. The ability of the present method to capture and preserve important flow features such as shockwave and vortex flow is shown in Fig. 15. In this figure continuous pressure contours are observed across the non-matching boundary indicating the preservation of the shockwave and the vortex flow originating from the strake.

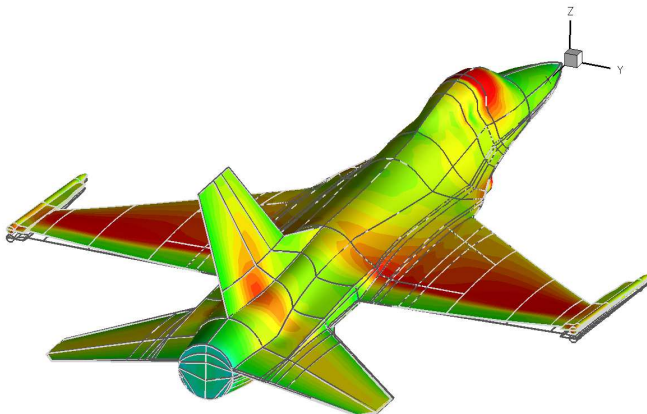


Fig. 16 Pressure distribution on the deformed surface of a fighter aircraft with dummy missiles at wing-tip flying at Mach 0.90, AOA 2 deg. and altitude of 5,000 ft

Finally, applications for static aeroelastic simulation are presented. Computations are carried out for an air to air configuration with only dummy missiles at station 1 and 9 and a configuration with Mark 84 bombs at stations 3 and 7, in addition to the dummy missiles at

stations 1 and 9. Static aeroelastic simulations are carried out at a Mach number of 0.90, an angle-of-attack of 2 degree and an altitude of 5,000 ft.

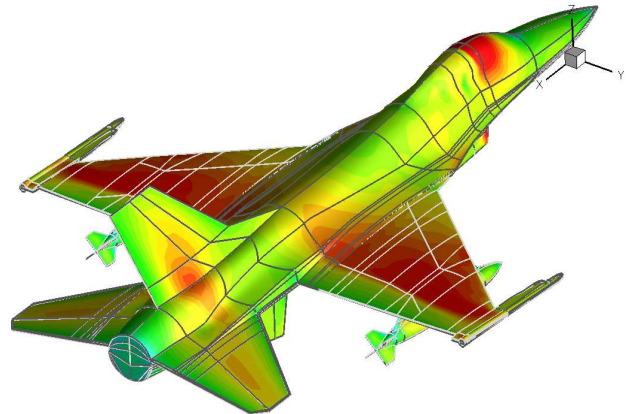


Fig. 17 Pressure distribution on the deformed surface of a fighter aircraft with dummy missiles at wing-tips and Mark 84 bombs at mid store attachments flying at Mach 0.90, AOA 2 deg. and altitude of 5,000 ft

The flexibility matrix for determining the structural deformation has been computed based on an assumption of a free-flying condition, i.e. the so called free-free flexibility matrix, see Ref. [3][11]. Fig. 16 and Fig. 17 present the surface pressure on the aircraft at the condition where both the flow equations and the structural deformation are converged. It can be seen that the inertia forces of the bomb prevent the wing to bend upward like in the case of the air-to-air configuration.

7 Conclusions and recommendations

A manoeuvre loads computation method suitable for military aircraft with multiple store configurations has been presented. The method relies on a non-matching boundary method to handle the store configurations easily and efficiently. Based on the results presented in this paper, the following conclusions may be drawn:

- verification test cases show that the error in approximating the variables of the ghost cells at non-matching boundary is relatively small,
- accurate results are obtained even for flows with shockwaves and vortices,

- best results are obtained when the grid stretching at the boundary is similar between the non-matching boundaries,
- the more efficient approach of using only a limited number of neighbouring cells for the interpolation does not reduce the accuracy of the results,
- the method can be applied in an aeroelastic simulation including surface and volume grid deformations.

Further it can be mentioned that the present modular approach relieves the burden of generating extremely complex grid for an aircraft with multiple store configurations.

Finally it is recommended to investigate further the variant of the interpolation method which can maintain the conservativity of the flow variables across non-matching boundaries.

8 References

- [1] Boelens, O.J., Goertz, S., Fritz, W. and Lamar, J. Description of the F16-XL Geometry and Computational Grids Used in CAWAPI. *Journal of Aircraft* 2009, vol 46, no. 2 (355-368).
- [2] Spiekhout, D.J., New Approach for Fatigue Life Monitoring RNLA F-16 Fleet, *Proceedings of the 1997 USAF ASIP Conference*, 1997.
- [3] Prananta, B.B., Meijer, J.J. and van Muijden, J. *Static aeroelastic simulation using CFD, comparison with linear method*. Paper presented at International Forum on Aeroelasticity and Structural Dynamics 2003, Amsterdam, 2003.
- [4] Prananta, B.B.; Veul, R.P.G., Houwink, R., Hounjet, M.H.L., Muijden, J. van, *A generic flexible aircraft loads database system for fatigue analysis*. Paper presented at International Forum on Aeroelasticity and Structural Dynamics 2007, Stockholm, Sweden.
- [5] Hounjet, M.H.L. and Meijer, J.J. *Evaluation of Elastomechanical and Aerodynamic Data Transfer Methods for Non-planar Configurations in Computational Aeroelastic Analysis*. Paper presented at International Forum on Aeroelasticity and Structural Dynamics 1995, also NLR TP 95690.
- [6] Baxter, B.J.C. *The interpolation theory of radial basis functions*. PhD thesis, Cambridge University, 1992.
- [7] J.H. van Tongeren, M.H.L. Hounjet, B.B. Prananta and B.J.G. Eussen. *Development of a fighter aircraft aeroelastic model based on an existing global-stress fem*. Paper presented at International Forum on Aeroelasticity and Structural Dynamics 2009, Seattle.
- [8] Prananta, B.B., Soemarwoto, B.I., Boelens, O.J., Kartika, B. and Chaedar, S. Analysis of store

separation from a generic twin-engine turboprop aircraft. AIAA-2007-4077, 25th AIAA Applied Aerodynamics Conference, Miami, Florida, June 25-28, 2007.

- [9] Rizzi, A, Jirásek, A., Lamar, J., Crippa, S., Badcock, K.J. and Boelens, O.J. Lessons Learned from Numerical Simulations of the F-16XL Aircraft at Flight Conditions. *Journal of Aircraft* 2009, vol.46 no.2 (423-441).
- [10] J.C Kok, J.W. Boerstoeel, A. Kassies, and S.P. Spekrijse. A robust multi-block navierstokesflow solver for industrial applications. NLR-TP-960503, NLR, Paper presented at Third ECCOMAS Computational Fluid Dynamics Conference, Paris, 1996
- [11] Rodden, W.P. and Johnson, E.H., *MSC/NASTRAN Aeroelastic analysis users's guide version 68*, MacNeal-Schwendler Corp, March 1994.
- [12] Spekrijse, Prananta, B.B. and Kok, J.C A simple, robust and fast algorithm to compute deformations of multi-block structured grids. NLR TP-2002-105, NLR.

Acknowledgement

The research presented in this paper is partly funded by the Netherlands Ministry of Defence and partly by the NLR through programmatic funding “Kennis als Vermogen”. The project monitor, Maj J. van der Laan, is acknowledged for his support. The presented non-matching boundary method is implemented in ENSOLV by dr. J.C. Kok and dr. H. van der Ven.

Contact Email Address

The authors can be contacted through the following email addresses: Bimo.Prananta@NLR.NL, Rudy.Veul@NLR.NL, Okko.Boelens@NLR.NL

Copyright Statement

The authors confirm that they, and/or their company or organization, hold copyright on all of the original material included in this paper. The authors also confirm that they have obtained permission, from the copyright holder of any third party material included in this paper, to publish it as part of their paper. The authors confirm that they give permission, or have obtained permission from the copyright holder of this paper, for the publication and distribution of this paper as part of the ICAS2010 proceedings or as individual off-prints from the proceedings.